Stability Analysis of Wide Area Damping Controllers with Multiple Time Delays ⋆

**Georgios Tzounas, Muyang Liu,
Mohammed Ahsan Adib Murad, Federico Milano**

*School of Electrical and Electronic Engineering,
University College Dublin, Ireland
{georgios.tzounas, muyang.liu, mohammed.murad}@ucdconnect.ie,
federico.milano@ucd.ie*

Abstract: The paper discusses the impact of multiple time delays on the stability of centralized wide area damping controllers (WADCs). These controllers are utilized in electric power systems to damp the interarea oscillations. With this aim, an ideal WADC is first designed based on the well-known H_∞ control scheme. Then delays are included for all remote signals of the WADC and different delay models, namely, constant, stochastic and periodic delays with dropout, are considered and compared. Both nonlinear time domain simulations and closed-loop eigenvalue analysis based on the 2-area test system are carried out. Finally, a probabilistic method to evaluate the impact of stochastic communication delays on small-signal stability is discussed.

Keywords: Interarea oscillations, wide area damping controller (WADC), H_∞ control, time delays, time domain integration, small-signal stability analysis (SSSA).

1. INTRODUCTION

1.1 Motivation

Electric energy networks are complex, nonlinear systems that include many control signals, some of which are transmitted over long distances. The communication of remote signals introduces time-varying stochastic delays that are known to impact on the stability of the overall power systems (Zhang and Bose, 2008; Wu et al., 2004). How to properly study the impact of such time-varying delays through accurate yet robust numerical techniques is still an open and challenging field of research and the objective of the present work.

1.2 Literature Review

Highly congested power systems often show poorly damped low frequency interarea oscillations. This problem has scaled in recent years due to the expansion of distribution networks, the penetration of renewable energy resources and an overall load increase.

The installation of Power System Stabilizers (PSSs) is a standard solution for damping electro-mechanical swings (Kundur, 1994). While they effectively reduce the impact of local modes of their synchronous machine, PSSs are often unable to damp the interarea oscillations (Zhang and Bose, 2008). The development of Wide Area Measurement Systems (WAMSs), in the past two decades, has introduced a new perspective in dealing with interarea oscillations. A WAMS is able to measure and process real-time dynamic data through Phasor Measurement Units (PMUs) (Kamwa et al., 2013). Wide area signals, that provide good or even global observability of the interarea modes, can be transmitted to a Wide Area Damping Controller (WADC) through a communication network (Wu et al., 2004). A variety of different strategies has been proposed in recent literature to design effective WADCs. Among these we cite single and multi-objective robust control synthesis (Yao et al., 2011), hierarchical structure (Okou et al., 2005), and adaptive critic controllers (Ray and Venayagamoorthy, 2008).

The involvement of the communication network in a WAMS introduces multiple delays, dropouts, disordering and noise in control signals delivery. However, the vast majority of existing studies has considered delays as constants. Only very recently more realistic time delays have been considered. In Wang et al. (2012), the impact of network-induced delays with data packet dropout and disordering on the control of wide area closed-loop power systems is studied. In Li and Chen (2017), Padhy et al. (2017), damping controllers that compensate realistic communication delays are designed. It is important to capture the actual behaviour of delays because constant and time-varying delays may affect the system stability unexpectedly, even if they are within the same range. This nonlinear behaviour is known as the *Quenching Phenomenon* (QP) (Papachristodoulou et al., 2007).

The impact of time delays on power system stability is not an easy task to solve. To this aim there are basically two broad approaches. Time domain and frequency domain analyses. The former is relatively easier to implement, provided that an appropriate implicit integration scheme

⋆ This work is supported by the Science Foundation Ireland, by funding Georgios Tzounas, Muyang Liu, Mohammed Ahsan Adib Murad and Federico Milano, under Investigator Programme Grant No. SFI/15/IA/3074. F. Milano is also supported by the European Community under the RESERVE Consortium (grant No. 727481).

is utilized (Bellen and Zennaro, 2003). Frequency domain approaches are also involved as they require the solution of a transcendental characteristic equation, with infinitely many roots and thus, only an approximation of the solution is possible (Milano and Anghel, 2012). In this paper, we consider both approaches.

In the literature, the impact of time delays on the stability of power systems has been mostly studied based on Lyapunov-Krasovskii Functionals (LKFs). Nevertheless, these functionals tend to be overconservative while time-domain and eigenvalue-based approaches appear delay-model dependent and, thus, are more adequate than LKFs to take into account the idiosyncrasies of time-varying delays (Liu and Milano, 2018). Comparison among eigenvalue-based methods have featured that the Chebyshev discretization of the partial differential equation representation of Delay Differential-Algebraic Equations (DDAEs) gives promising results (Liu et al., 2018). For this reason, the Chebyshev discretization is also utilized in this work.

1.3 Contributions

The novel contributions of the paper are as follows.

- A thorough comparison of the impact on transient and small-signal stability of constant and time-varying stochastic delays in centralized WADCs. This extends the results obtained in (Liu et al., 2018), where only decentralized PSSs are considered.
- A Monte Carlo-based technique that attempts to define the small-signal stability of time-varying delays through stochastically distributed constant delays.

1.4 Organization

The remainder of the paper is organized as follows. Section 2 outlines the dynamic model of power systems and the implemented WADC scheme based on H_∞ control. Section 3 recalls the mathematical background to study the stability of a set of DDAEs and describes the constant and time-varying stochastic delay models considered in this work. The case study is discussed in Section 4 through time-domain simulations and small-signal stability analysis (SSSA) based on the well-known 2-area system (Kundur, 1994). The sensitivity of the damping performance to the delay models, the closed-loop stability and a method to improve the constant delay results are also discussed in Section 4. Finally, in Section 5 the main results of the paper are summarized and conclusions are duly drawn.

2. POWER SYSTEM AND WADC MODELS

2.1 Modeling of power systems

Power systems can be described through a set of Differential Algebraic Equations (DAEs):

$$\begin{aligned} \dot{\boldsymbol{x}} &= \boldsymbol{f}(\boldsymbol{x}, \boldsymbol{y}, \boldsymbol{d}, \boldsymbol{u}) \\ \boldsymbol{0} &= \boldsymbol{g}(\boldsymbol{x}, \boldsymbol{y}, \boldsymbol{d}, \boldsymbol{u}) \ , \end{aligned} \tag{1}$$

where $\boldsymbol{f}$ ($\boldsymbol{f} : \mathbb{R}^{n+m+q+p} \rightarrow R^n$) are the differential equations, $\boldsymbol{g}$ ($\boldsymbol{g} : \mathbb{R}^{n+m+q+p} \rightarrow R^m$) are the algebraic equations, $\boldsymbol{x}$, $\boldsymbol{x} \in \mathbb{R}^n$, and $\boldsymbol{y}$, $\boldsymbol{y} \in \mathbb{R}^m$, are the state and algebraic variables, respectively; $\boldsymbol{d}$, $\boldsymbol{d} \in \mathbb{R}^q$, are uncontrollable inputs, e.g., noise and load variations; and $\boldsymbol{u}$, $\boldsymbol{u} \in \mathbb{R}^p$, are the controlled inputs, e.g., regulator input references. Differentiating (1) around an equilibrium point gives:

$$\begin{aligned} \dot{\boldsymbol{x}} &= \boldsymbol{f_x}\Delta\boldsymbol{x} + \boldsymbol{f_y}\Delta\boldsymbol{y} + \boldsymbol{f_d}\Delta\boldsymbol{d} + \boldsymbol{f_u}\Delta\boldsymbol{u} \\ \boldsymbol{0} &= \boldsymbol{g_x}\Delta\boldsymbol{x} + \boldsymbol{g_y}\Delta\boldsymbol{y} + \boldsymbol{g_d}\Delta\boldsymbol{d} + \boldsymbol{g_u}\Delta\boldsymbol{u} \ , \end{aligned} \tag{2}$$

where $\boldsymbol{f_x}$, $\boldsymbol{f_y}$, $\boldsymbol{f_d}$, $\boldsymbol{f_u}$, $\boldsymbol{g_x}$, $\boldsymbol{g_y}$, $\boldsymbol{g_d}$, and $\boldsymbol{g_u}$ are the system Jacobian matrices. The state matrix $\boldsymbol{A}$ is obtained with the elimination of algebraic variables from (2):

$$\Delta\dot{\boldsymbol{x}} = \boldsymbol{A}\Delta\boldsymbol{x} + \boldsymbol{B}_1\Delta\boldsymbol{d} + \boldsymbol{B}_2\Delta\boldsymbol{u} \ , \tag{3}$$

where $\boldsymbol{A} = \boldsymbol{f_x} - \boldsymbol{f_y}\boldsymbol{g_y}^{-1}\boldsymbol{g_x}$, $\boldsymbol{B}_1 = \boldsymbol{f_d} - \boldsymbol{f_y}\boldsymbol{g_y}^{-1}\boldsymbol{g_d}$ and $\boldsymbol{B}_2 = \boldsymbol{f_u} - \boldsymbol{f_y}\boldsymbol{g_y}^{-1}\boldsymbol{g_u}$. The form of (3) leads to a much simpler and more conventional state space representation of the Multiple-Input Multiple-Output (MIMO) system as described in the next section. However, the matrices that appear in (2) are much sparser than $\boldsymbol{A}$, $\boldsymbol{B}_1$ and $\boldsymbol{B}_2$, and hence (2) is the form utilized in the software implementation numerical analysis carried out in this paper.

2.2 H_∞ Control Scheme

The well-known H_∞ control is basically an optimization problem that synthesizes a stabilizing controller $\boldsymbol{K}(s)$ which minimizes the H_∞ norm of the closed-loop transfer matrix from the disturbance $\boldsymbol{d}$ to the output $\boldsymbol{z}$ for a given open loop plant $\boldsymbol{P}(s)$ through the measurements $\boldsymbol{w}$ (see Fig. 1). In general, $\boldsymbol{z}$ and $\boldsymbol{w}$ are nonlinear functions of a subset of the system variables.

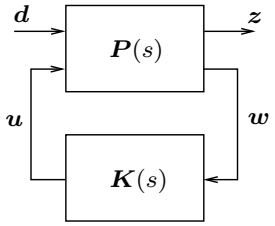

Fig. 1. Block diagram of the H_∞ control scheme.

The minimization of the H_∞ norm implies the minimization of the maximum energy amplification ratio between $\boldsymbol{d}$ and $\boldsymbol{z}$. The MIMO state space realization of $\boldsymbol{P}(s)$ is

$$\begin{aligned} \Delta\dot{\boldsymbol{x}} &= \boldsymbol{A}\Delta\boldsymbol{x} + \boldsymbol{B}_1\Delta\boldsymbol{d} + \boldsymbol{B}_2\Delta\boldsymbol{u} \\ \Delta\boldsymbol{z} &= \boldsymbol{C}_1\Delta\boldsymbol{x} + \boldsymbol{D}_{11}\Delta\boldsymbol{d} + \boldsymbol{D}_{12}\Delta\boldsymbol{u} \\ \Delta\boldsymbol{w} &= \boldsymbol{C}_2\Delta\boldsymbol{x} + \boldsymbol{D}_{21}\Delta\boldsymbol{d} + \boldsymbol{D}_{22}\Delta\boldsymbol{u} \end{aligned} \tag{4}$$

The following assumptions are made (Zhou and Doyle, 1998):

(1) For the existence of stabilizing controllers, the pairs ($\boldsymbol{A}$, $\boldsymbol{B}_2$) and ($\boldsymbol{C}_2$, $\boldsymbol{A}$) must be stabilizable and detectable, respectively.
(2) $\boldsymbol{D}_{12}$, $\boldsymbol{D}_{21}$ must be left and right invertible, respectively. This means that the penalty on $\boldsymbol{z}$ includes a non-singular penalty on the control $\boldsymbol{u}$ and that the measurement signal $\boldsymbol{w}$ includes non-singular plant disturbance.
(3) The matrices

$$\begin{bmatrix} \boldsymbol{A} - j\omega\boldsymbol{I} & \boldsymbol{B}_2 \\ \boldsymbol{C}_1 & \boldsymbol{D}_{12} \end{bmatrix}, \text{ and } \begin{bmatrix} \boldsymbol{A} - j\omega\boldsymbol{I} & \boldsymbol{B}_1 \\ \boldsymbol{C}_2 & \boldsymbol{D}_{21} \end{bmatrix}$$

must be left and right invertible, respectively, $\forall \omega \in R$.

The structure of the resulting controller feedback dynamic gain $\boldsymbol{K}(s)$ in Fig. 1 is:

$$\begin{aligned} \Delta \dot{\boldsymbol{x}}_{\boldsymbol{c}} &= \boldsymbol{A}_c \Delta \boldsymbol{x}_c + \boldsymbol{B}_c \Delta \boldsymbol{w} \\ \Delta \boldsymbol{u} &= \boldsymbol{C}_c \Delta \boldsymbol{x}_c + \boldsymbol{D}_c \Delta \boldsymbol{w} \ . \end{aligned} \tag{5}$$

2.3 Design of the WADC

In this study, the disturbance $\boldsymbol{d}$ is a step variation of the field voltage (v_f) of a given synchronous machine. The measurement signal $\boldsymbol{w}$ is selected as the frequency deviation at the point of common connection of the generator and the grid:

$$\Delta \omega = \omega - \omega^{\text{ref}} \ . \tag{6}$$

As discussed above, $\boldsymbol{w}$ also includes full measurement noise that depends on the disturbance $\boldsymbol{d}$. The control signal is considered as an additional input to the Automatic Voltage Regulator (AVR) reference (see Fig. 2):

$$v^{\text{ref}} = v_0^{\text{ref}} + v_{\text{wadc}} \ . \tag{7}$$

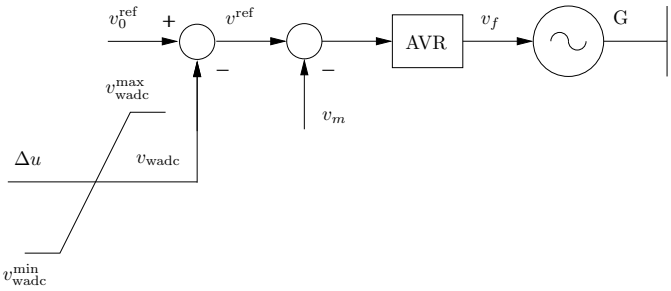

Fig. 2. Block diagram of applied control.

Finally, the output $\boldsymbol{z}$ includes the speed deviation of the machines, with the aim of drastically damping the electromechanical oscillations.

The following remarks are relevant:

- The use of geometric measures of controllability/ observability is probably the best method to select the most effective stabilizing signals and control locations (Heniche and Kamwa, 2008).
- The design of a dynamic controller and/or its formulation as a Linear Matrix Inequalities (LMI) problem with a number of constraints would be likely to give better damping of the swings.

Other choices for $\boldsymbol{d}$, $\boldsymbol{z}$ and $\boldsymbol{w}$ are possible. However, the development of a novel WADC is out of the scope of this paper. Rather, the focus is on a systematic analysis of the impact of approximated and accurate delay models on the stability of the overall system including the WADC. For the sake of comparison, we utilize a set of $\boldsymbol{d}$, $\boldsymbol{z}$ and $\boldsymbol{w}$ that have been considered in the literature and proved to work well when no delays are considered.

3. DDAES AND DELAYS MODELING

The resulting closed-loop system combines (1) and (5) plus the expressions of the measurements $\boldsymbol{w}$, hence, the vector of state and algebraic variables becomes $\hat{\boldsymbol{x}} = (\boldsymbol{x}, \boldsymbol{x}_c)$ and $\hat{\boldsymbol{y}} = (\boldsymbol{y}, \boldsymbol{u}, \boldsymbol{w})$, respectively. Introducing time delays in the closed-loop system, changes the DAEs into a set of DDAEs. The index-1 Hessenberg form is adequate to model power systems with delays (Milano and Anghel, 2012):

$$\begin{aligned} \dot{\hat{\boldsymbol{x}}} &= \hat{\boldsymbol{f}}(\hat{\boldsymbol{x}}, \hat{\boldsymbol{y}}, \hat{\boldsymbol{x}}_d, \hat{\boldsymbol{y}}_d) \\ \boldsymbol{0} &= \hat{\boldsymbol{g}}(\hat{\boldsymbol{x}}, \hat{\boldsymbol{y}}, \hat{\boldsymbol{x}}_d) \ , \end{aligned} \tag{8}$$

where $\hat{\boldsymbol{x}}_d$ and $\hat{\boldsymbol{y}}_d$ are the delayed state variables and algebraic variables, respectively. Since $\boldsymbol{d}$ and $\boldsymbol{z}$ are only utilized for the definition of (5), they are not included in the expression of (8). Linearization around the operating point gives:

$$\begin{aligned} \dot{\hat{\boldsymbol{x}}} &= \hat{\boldsymbol{f}}_{\hat{\boldsymbol{x}}} \Delta \hat{\boldsymbol{x}} + \hat{\boldsymbol{f}}_{\hat{\boldsymbol{y}}} \Delta \hat{\boldsymbol{y}} + \hat{\boldsymbol{f}}_{\hat{\boldsymbol{x}}_d} \Delta \hat{\boldsymbol{x}}_d + \hat{\boldsymbol{f}}_{\hat{\boldsymbol{y}}_d} \Delta \hat{\boldsymbol{y}}_d \\ \boldsymbol{0} &= \hat{\boldsymbol{g}}_{\hat{\boldsymbol{x}}} \Delta \hat{\boldsymbol{x}} + \hat{\boldsymbol{g}}_{\hat{\boldsymbol{y}}} \Delta \hat{\boldsymbol{y}} + \hat{\boldsymbol{g}}_{\hat{\boldsymbol{x}}_d} \Delta \hat{\boldsymbol{x}}_d \ , \end{aligned} \tag{9}$$

where $\hat{\boldsymbol{f}}_{\hat{\boldsymbol{x}}_d}$, $\hat{\boldsymbol{f}}_{\hat{\boldsymbol{y}}_d}$, $\hat{\boldsymbol{g}}_{\hat{\boldsymbol{x}}_d}$ are the delayed Jacobian matrices. For the general case of multiple, time-varying delays, after the elimination of algebraic variables $\hat{\boldsymbol{y}}$ and $\hat{\boldsymbol{y}}_d$, we obtain:

$$\dot{\hat{\boldsymbol{x}}}(t) = \hat{\boldsymbol{A}}_0 \hat{\boldsymbol{x}}(t) + \sum_{i=1}^{r} \hat{\boldsymbol{A}}_i \hat{\boldsymbol{x}}(t - \tau_i(t)) \ , \tag{10}$$

where $r \in \mathbb{N}^+$; $\tau_i(t) : \mathbb{R}^+ \to [\tau_{\min}, \tau_{\max}], 0 \leq \tau_{\min} < \tau_{\max}$.

In a WAMS, delays exist both in the input network measurement units - controller ($\boldsymbol{w}$) and the output network controller - local actuators ($\boldsymbol{u}$). In the following, without loss of generality, delays are included only in the measurement variables $\boldsymbol{w}$.

The time-varying delays are modelled as:

$$\tau_i(t) = \tau_{0,i} + \tau_{p,i}(t) + \tau_{s,i}(t) \ , \tag{11}$$

where:

- The constant component $\tau_{0,i}$ expresses the processing time of the measurement unit plus the inevitable delay imposed by the communication medium.
- The periodic component $\tau_{p,i}(t)$ implies that the data packets are sent repeatedly in discrete time instants.
- The stochastic part $\tau_{s,i}(t)$ includes uncertainties and noises during the transmission, as well as the probability of a dropout.

An example of time-varying delay is shown in Fig. 3. The interested reader can find more detail on this model in Liu et al. (2018).

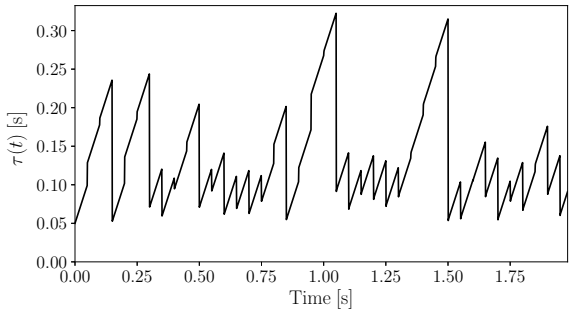

Fig. 3. Realistic WAMS delay.

4. CASE STUDY

The test system employed for our simulations is illustrated in Fig. 4. This system has been set up to show significant interarea oscillations (Kundur, 1994) and thus, has been

widely deployed in studies of this kind. It consists of 2 areas connected through bus 8, 11 buses and 4 generators connected at the medium voltage level of 20 kV, while the high voltage transmission system operates at 230 kV.

Frequency measurements are periodically sent from the measurement units installed on the four terminal buses of the generating units. The WADC implements the H_∞ optimization and the output control signals are sent to the respective AVRs, as described in Section 2. Based on the discussion given in Section 3, the WADC includes four time delays and the time dependency $\tau_i(t)$ of each delay is given by (11).

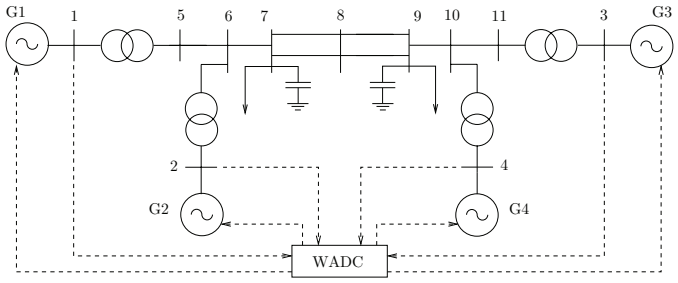

Fig. 4. Two-area four-machine test system.

All simulations in this Section were carried using Dome, a Python-based software tool for power system analysis (Milano, 2013).

4.1 Time-Domain Simulation

The tripping of one of the high voltage transmission lines that connects buses 7 and 8 is considered. The contingency occurs at $t_1 = 0.2$ s and the normal operation is restored at $t_2 = 0.3$ s. In Figs. 5 - 7, the angle frequency of G1 (ω_1) is plotted for different scenarios.

Figure 5 shows the effect of the applied contingency with and without WADC and no delays. In the ideal case of instantaneous transmission of the signals, the damping of electro-mechanical oscillations is significantly improved with the addition of the WADC. This ideal scenario serves as a reference for the remainder of this section.

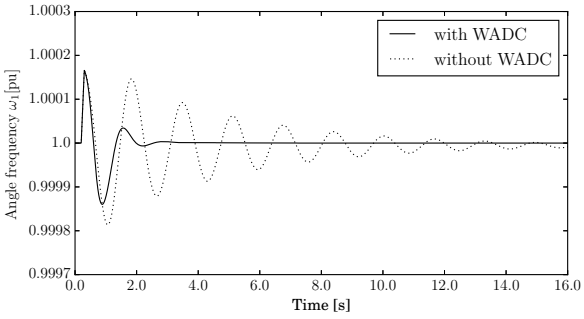

Fig. 5. Rotor speed of G1 with delay-free WADC and without WADC.

The following constant delay scenarios are considered next:

- All delays have equal magnitudes, τ_0.
- The delays have different magnitudes and their mean value is $\bar{\tau} = \tau_0$.

Simulation results are presented in Fig. 6. The magnitude of the equal delays in this case is $\tau_0 = 180$ ms. The different constant delays vary from 90 to 270 ms. In both scenarios, the electro-mechanical swings are poorly damped. In this case, however, the equal delay scenario is more conservative. It is thus important to consider multiple-delay DDAEs, as considering a unique delay for all measured signals of the system can lead to inaccurate results.

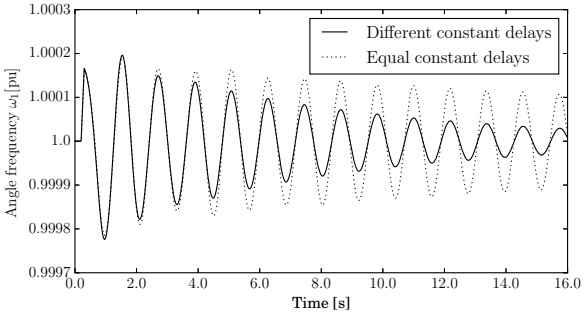

Fig. 6. Rotor speed of G1 with equal and different constant delays ($\bar{\tau} = 180$ ms).

We now consider realistic time-varying delays, as in (11). Based on (Liu et al., 2018), we assume that each delay has a constant component 130 ms, a periodic component with frequency 20 Hz and a stochastic component determined by a Gamma distribution with shape and scale parameters $k = 2$ and $\theta = 0.02$, respectively. Moreover, the periodic part of the delay is assumed to have 10% data dropout rate. The expected value of the resulting delay is 200 ms.

The rotor speed G1 is shown in Fig. 7. The realistic WAMS delay and constant delay scenarios are compared. For the constant delay scenario, $\tau_0 = 200$ ms is assumed for all signals. In this case, the constant delay model shows a negative damping, while the system with the realistic WAMS delays is stable, although poorly damped.

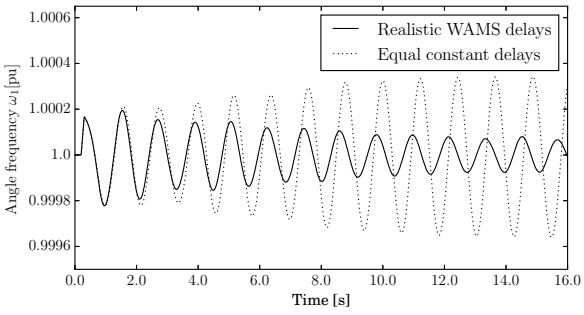

Fig. 7. Rotor speed of G1 for realistic WAMS delays ($\bar{\tau} = 200$ ms).

From the results obtained in Figs. 5-7, the following observations are relevant:

- The introduction of the signal delays, no matter what model is assumed for the delays, deteriorates the performance of the WADC.
- The equal constant delay model is the most conservative of the considered scenarios. Based on the

observation of Fig. 7, this may lead to assume even that the system is unstable even when it is not.

4.2 Small-Signal Stability Analysis

The time domain simulation, while it allows considering detailed delay models, can be time consuming, especially if sensitivity and/or Monte Carlo analyses are considered. These can be conveniently evaluated through a closed-loop SSSA.

The rightmost eigenvalues for the scenario of equal constant (180 ms) delays is shown in Fig. 8. The system presents three pairs of poorly damped eigenvalues.

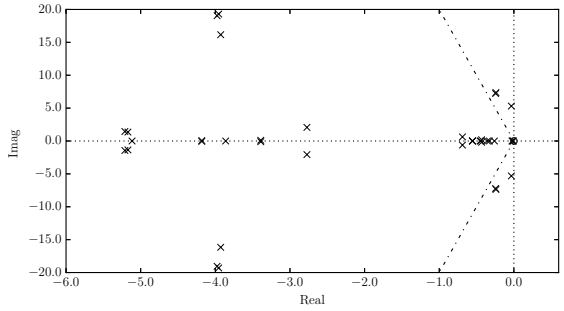

Fig. 8. Rightmost eigenvalues for the 2-area system with WADC and equal constant delays (180 ms).

The eigenvalue analysis is conducted several times by increasing τ_0. Figure 9 compares the real part of the complex dominant eigenvalue for equal constant and stochastic WAMS delays.

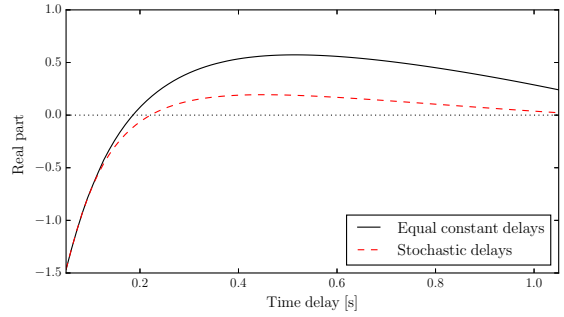

Fig. 9. Real part of the dominant eigenvalue $\mathrm{Re}\{\lambda_c\}$ for equal constant delays and stochastic WAMS delays as τ_0 varies.

For both models, the real part of the critical mode $\mathrm{Re}\{\lambda_c\}$ exhibits a maximum with respect to τ_0. The most unfavourable conditions for the stability of the system are for $\tau_0 = 450$ ms and $\tau_0 = 500$ ms for the stochastic and constant models, respectively. The results obtained with the constant delays model is always more conservative than the detailed model in the region of τ_0 that is typical of WADC, i.e., for $\tau_0 > 100$ ms.

The constant delays model is clearly attractive for the relative simplicity of its implementation. On the other hand, the realistic WAMS delay model, while accurate, is mathematically more involved and numerically less robust. It is worth noticing, in fact, that to obtain the dashed line shown in Fig. 9 is not straightforward. To this aim, we have utilized a Newton correction method that refines the approximated results obtained with the approximation of the time varying delays as distributed delays (Liu et al., 2018). The ability to converge to the correct eigenvalue and the accuracy of such a technique highly depends on the initial guess made for the delays and their eigenvectors. The larger the value of τ_o, the more difficult to find an adequate initial guess.[1] For this reason, the stochastic WAMS model plotted in Fig. 9 uses a simplified version of the realistic model presented in Section 3, without the periodic component, the addition of which would make the analysis untractable.

4.3 Monte Carlo SSSA with Constant Delays

Section 4.1 discusses the effect of multiple constant delays with unequal magnitudes on the performance of the WADC. In this section, we further elaborate on this scenario by assuming that the four delays are constant in a given period, but that their values are stochastically distributed following a Gamma distribution. A Monte Carlo stability analysis is carried out based on 4000 simulations for different magnitudes of delays.

The results are summarized in Table 1. The system is always stable for $\bar{\tau} = 100$ ms. For $\bar{\tau} = 200$ ms, the system is stable for the stochastic WAMS delays and unstable for equal constant delays. The stochastically distributed delay model reduces the conservativeness obtained with the equal delay model, as the system is expected to be stable with a probability of 29.30%. For higher $\bar{\tau}$, the system becomes unstable for both equal constant and stochastic WAMS delays (see Fig. 9). The stochastically distributed delay model captures the instability in 99.65% and 99.77% of the simulations for $\bar{\tau} = 300$ and $\bar{\tau} = 400$ ms, respectively.

Table 1. Monte Carlo SSSA.

θ	0.01	0.02	0.03	0.04
$\bar{\tau} = k \cdot \theta$ [s]	0.1	0.2	0.3	0.4
% stable	100.00	29.30	0.35	0.23

Finally, we consider the distribution of the real part of the most critical eigenvalue $\mathrm{Re}\{\lambda_c\}$ for $k = 10$, $\theta = 0.04$ and $\bar{\tau} = 400$ ms. The probability density and the cumulative probability of $\mathrm{Re}\{\lambda_c\}$ as obtained with the Monte Carlo method are shown in Figs. 10 and 11.

The obtained histogram in Fig. 10 is asymmetrical. It is calculated that:

$$P(0.189 \leq \mathrm{Re}\{\lambda_c\} \leq 0.534) = 92.38\% \ ,$$

which is the probability that $\mathrm{Re}\{\lambda_c\}$ falls between 0.189 and 0.534, which are the values of $\mathrm{Re}\{\lambda_c\}$ for the realistic WAMS delay and the equal constant delay models according to Fig. 9. This results can be interpreted as the probability that the configuration of the multiple unequal delays reduces the conservativeness of the equal constant delays model.

[1] We have utilized a 4^{th} order Padé approximant for the definition of the initial guesses.

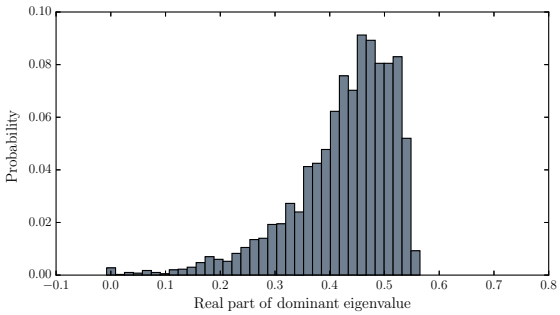

Fig. 10. Probability density of $\mathrm{Re}\{\lambda_c\}$.

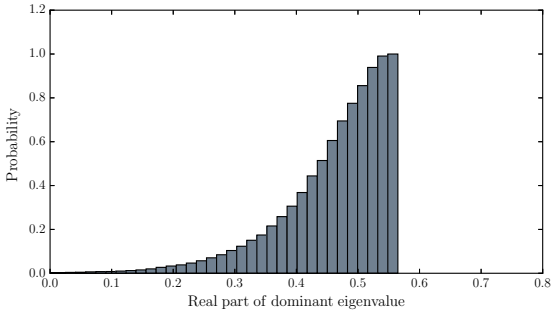

Fig. 11. Cumulative probability of $\mathrm{Re}\{\lambda_c\}$.

5. CONCLUSION

The paper discusses the impact of multiple time delays on the dynamic performance of a centralized WADC and the stability of the overall power system. This performance is evaluated through time domain simulations, while the impact of time delays on the system stability is studied through a SSSA and considering several scenarios.

As expected, typical communication delays of the order of few hundreds of milliseconds lead to potentially poorly damped and even unstable WADCs. A novel result of this paper is that the difference between poor damping and instability highly depends on the model of the delay.

The conventional and widely utilized model that considers the same constant delay for all measured signals appears to be quite conservative with respect to a precise representation of the time-varying and stochastic components that characterize communication delays. Unfortunately, the numerical volatility of the realistic delay model makes its utilization a time consuming challenge.

The probabilistic analysis approach that considers a Monte Carlo method and constant stochastic delays following a Gamma distribution appears as a promising compromise between accuracy and numerical robustness. We will dedicate future work to further develop this approach.

REFERENCES

Bellen, A. and Zennaro, M. (2003). *Numerical Methods for Delay Differential Equations*. Oxford Science Publications, Oxford.

Heniche, A. and Kamwa, I. (2008). Assessment of two methods to select wide-area signals for power system damping control. *IEEE Trans. on Power Systems*, 23(2), 572–581.

Kamwa, I., Samantaray, S.R., and Joos, G. (2013). Optimal integration of disparate C37.118 PMUs in wide-area PSS with electromagnetic transients. *IEEE Trans. on Power Systems*, 28(4), 4760–4770.

Kundur, P. (1994). *Power system stability and control*. Mc-Grall Hill, New York.

Li, M. and Chen, Y. (2017). A wide-area dynamic damping controller based on robust H_∞ control for wide-area power systems with random delay and packet dropout. *IEEE Trans. on Power Systems*, PP(99), 1–1.

Liu, M., Dassios, I., Tzounas, G., and Milano, F. (2018). Stability analysis of power system with inclusions of realistic wide-area measurement delay. *IEEE Trans. on Power Systems*. Under review, availabe at http://faraday1.ucd.ie/archive/papers/wamsdelay.pdf.

Liu, M. and Milano, F. (2018). Small-signal stability analysis of power systems with inclusion of periodic time-varying delays. In *Proceedings of the 20th PSCC*. Dublin, Ireland.

Milano, F. (2013). A Python-based Software Tool for Power System Analysis. In *Procs of the IEEE PES General Meeting*. Vancouver, BC.

Milano, F. and Anghel, M. (2012). Impact of time delays on power system stability. *IEEE Trans. on Circuits and Systems - I: Regular Papers*, 59(4), 889–900.

Okou, F., Dessaint, L., and Akhrif, O. (2005). Power systems stability enhancement using a wide-area signals based hierarchical controller. *IEEE Trans. on Power Systems*, 20(3), 1465–1477.

Padhy, B.P., Srivastana, S.C., and Verma, N. (2017). A wide-area damping controller considering network input and output delays and packet drop. *IEEE Trans. on Power Systems*, 32(1), 166–176.

Papachristodoulou, A., Peet, M.M., and Niculescu, S. (2007). Stability analysis of linear system with time-varying delays: Delay uncertainty and quenching. In *Procs of the 46th IEEE Conference on Decision and Control*. New Orleans, LA. USA.

Ray, S. and Venayagamoorthy, G.K. (2008). Real-time implementation of a measurement-based adaptive wide-area control system considering communication delays. *IET Generation, Transmission & Distribution*, 2(1), 62–70.

Wang, S., Meng, X., and Chen, T. (2012). Wide-area control of power systems through delayed network communication. *IEEE Trans. on Control Systems Technology*, 20(2), 495–503.

Wu, H., Tsakalis, K.S., and Heydt, G.T. (2004). Evaluation of time delay effects to wide-area power system stabilizer design. *IEEE Trans. on Power Systems*, 19(4), 1935–1941.

Yao, W., Jiang, L., Wu, Q.H., Wen, J.Y., and Cheng, S.J. (2011). Delay-dependent stability analysis of the power system with a wide-area damping controller embedded. *IEEE Trans. on Power Systems*, 26(1), 233–240.

Zhang, Y. and Bose, A. (2008). Design of wide-area damping controllers for interarea oscillations. *IEEE Trans. on Power Systems*, 23(3), 1136–1143.

Zhou, K. and Doyle, J.C. (1998). *Essentials of robust control*. Prentice Hall.

This Article is part of a project that has received funding from the **European Union's Horizon 2020 research and innovation programme under grant agreement Nº727481**